An Integrative Approach Using Phylogenomics and High-Resolution X-Ray Computed Tomography for Species Delimitation in Cryptic Taxa

KIRILEE CHAPLIN[1,2], JOANNA SUMNER[1], CHRISTY A. HIPSLEY[1,2], AND JANE MELVILLE[1,*]

[1]*Department of Sciences, Museums Victoria, GPO Box 666, Melbourne, Victoria 3001, Australia; and* [2]*School of BioSciences The University of Melbourne Parkville Campus Victoria 3010, Australia*
Correspondence to be sent to: Department of Sciences, Museums Victoria, GPO Box 666, Melbourne, Victoria 3001, Australia;
E-mail: jmelv@museum.vic.gov.au.

Abstract.—Morphologically cryptic taxa have proved to be a long-standing challenge for taxonomists. Lineages that show strong genomic structuring across the landscape but are phenotypically similar pose a conundrum, with traditional morphological analyses of these cryptic lineages struggling to keep up with species delimitation advances. Micro X-ray computed tomography (CT) combined with geometric morphometric analyses provides a promising avenue for identification of morphologically cryptic taxa, given its ability to detect subtle differences in anatomical structures. However, this approach has yet to be used in combination with genomic data in a comparative analytical framework to distinguish cryptic taxa. We present an integrative approach incorporating genomic and geometric morphometric evidence to assess the species delimitation of grassland earless dragons (*Tympanocryptis* spp.) in north-eastern Australia. Using mitochondrial and nuclear genes (ND2 and RAG1, respectively), along with >8500 SNPs (nuclear single nucleotide polymorphisms), we assess the evolutionary independence of target lineages and several closely related species. We then integrate phylogenomic data with osteological cranial variation between lineages using landmark-based analyses of three-dimensional CT models. High levels of genomic differentiation between the three target lineages were uncovered, also supported by significant osteological differences. By incorporating multiple lines of evidence, we provide strong support for three undescribed cryptic lineages of *Tympanocryptis* in north-eastern Australia that warrant taxonomic review. Our approach demonstrates the successful application of CT with integrative taxonomic approaches for cryptic species delimitation, which is broadly applicable across vertebrates containing morphologically similar yet genetically distinct lineages. Additionally, we provide a review of recent integrative taxonomic approaches for cryptic species delimitation and an assessment of how our approach can value-add to taxonomic research. [Geometric morphometrics; grassland earless dragons; integrative taxonomy; micro X-ray computed tomography; phylogenomics; SNPs; species delimitation; *Tympanocryptis*.]

Molecular taxonomy (using genetic techniques for species delimitation) has been on the rise over the past three decades (Moritz and Cicero 2004; Vogler and Monaghan 2007), leading to an exponential increase in lineage delimitation or species descriptions that are predominately molecular-based (e.g., Gottscho et al. 2017; Singhal et al. 2018; Esquerré et al. 2019). In the last few years, an increasing number of studies predicate taxonomic decisions on genomic data (Coates et al. 2018). Many of these studies demonstrate that population-level genomic assays can reveal fine-scale geographic structuring in species complexes, increasing the difficulty in determining whether variation is at the species or population level. Consequently, there is a risk of over-splitting species in taxonomic treatments based on genomic data (Coates et al. 2018) and there is ongoing criticism of the validity of genetically distinct lineages with little to no morphological variation being elevated to species level (Lipscomb et al. 2003; Will and Rubinoff 2004; Hebert and Gregory 2005; Vogler and Monaghan 2007; Kvist 2013).

Whole-evidence species delimitation, integrating genomic data with other lines of evidence (e.g., morphological, ecological), has been proposed as an optimal approach to species delimitation in the genomic age (Dayrat 2005; Fišer et al. 2018). Whole-evidence approaches to species delimitation in taxonomy, known as integrative taxonomy, are not new (e.g., Dayrat 2005; Padial et al. 2010; Wielstra and Arntzen 2014); however,

the field of integrative taxonomy is entering a new era, with the greater accessibility to genomic techniques and comparative evolutionary analyses (Padial et al. 2010; McKay et al. 2014; Fišer et al. 2018). Recently, there have been a number of studies proposing workflows and methods that integrate traditional morphology with genomic data using comparative analytical approaches to increase confidence in species delimitation decisions (e.g., Pyron et al. 2016; Singhal et al. 2018).

One area of taxonomy to which such whole-evidence approaches will be particularly powerful as we move into the genomic age is the phenomenon of cryptic species (Papakostas et al. 2016). Cryptic species occur when daughter species accumulate genetic differences without apparent morphological divergence, resulting in phenotypic similarities (Bickford et al. 2007; Mathews et al. 2002; Smith et al. 2011). A recent review has highlighted the difference between conceptual and operational issues when addressing cryptic species (Fišer et al. 2018), detailing the importance of further research in both these areas. Our study addresses operational difficulties of delimitation between cryptic lineages in the description and naming of species.

Cryptic lineages highlight the complexities of phenotypic evolution (Bruna et al. 1996) and have continued to provide difficulties for systematists and taxonomists in determining true species diversity. Recent studies,

using comparative analytical approaches to integrate traditional morphological data with phylogenomics, have provided a significant step forward in the tools available for taxonomic decision-making. However, quantifying morphological variation within cryptic species complexes using traditional external traits often results in no detectable differences (e.g., Singhal et al. 2018), meaning that once again taxonomic decisions are based predominantly on the genomic data. In such cases, high-resolution genomic data are typically combined with lower resolution phenotypic data related to size (e.g., body length, width, mass), meaning few independent variables despite many measurements.

Fortunately, alternative methods known as geometric morphometrics (GM) now allow biologists to extract high-resolution phenotypic data from organisms and to integrate those data into a phylogenetic framework. In contrast to traditional measurements, this approach uses anatomically defined landmarks, or points, to describe biological shape after variation in specimen position, orientation, and scale have been removed (for a GM overview, see Adams et al. 2013). The resulting multivariate data can be conditioned on a phylogeny to, among other things, visualize evolutionary trends in morphospace (i.e., phylomorphospace; Sherratt et al. 2014), estimate the degree to which phenotypic similarity is associated with relatedness (i.e., phylogenetic signal; Adams 2014a), and evaluate group structure and covariation between shape and other variables (Adams 2014b; Collyer et al. 2015). Studies incorporating GM with molecular data to distinguish cryptic taxa have so far focused on single genes and two-dimensional (Milankov et al. 2009; Abdelaziz et al. 2011; Karanovic et al. 2016; Kordbacheh et al. 2018) or three-dimensional (Gabelaia et al. 2018; Caro et al. 2019) landmarks. In most of these cases, sampled individuals for morphology and genetics differed, making their taxonomic affinities difficult to ascertain. To our knowledge, 3D landmark-based GM has yet to be used with whole-genome sequencing in an integrative taxonomic framework.

Here, we provide a new approach for taxonomic decisions of species delimitation in cryptic taxa that combines phylogenomic and morphological data in a comparative framework. Following a step-down procedure, we integrate evidence from phylogeographic and phylogenomic data with geometric morphometric analyses of 3D X-ray computed tomographic (CT) osteological models. For the initial step, we use broad geographic screening based on mtDNA and nuclear genes, common in molecular taxonomy (e.g., Shoo et al. 2008; Melville et al. 2014), to identify samples to be included in the workflow. These phylogeographic data provide a baseline understanding of geographic-based genetic structure, broadly comparable to existing studies that use similar single mtDNA and nuclear gene techniques for cryptic taxa delimitation (Oliver et al. 2007). We then utilize genomic data through a genome complexity reduction method that uses a restriction-enzyme based pipeline to generate single nucleotide polymorphism (SNP) libraries (Jaccoud et al. 2001; Cruz et al. 2013) to provide a robust phylogenomic framework for identifying evolutionary lineages (Morin et al. 2004; Van Tassell et al. 2008; Kumar et al. 2012; Melville et al. 2017). Geometric morphometric analyses of the CT models are then performed on the same samples used in the phylogenomic section of the workflow. This approach provides matching genomic and morphological data for the samples. Finally, we use a comparative analytical approach to integrate phylogenomic data with the geometric morphometric results to delimit cryptic taxa.

We apply this step-down approach to species delimitation in Australian earless dragons (Agamidae: *Tympanocryptis* spp.); a group with unclear systematics and unresolved taxonomy due to the presence of cryptic lineages (Smith et al. 1999; Melville et al. 2007; Doughty et al. 2015; Melville et al. 2014). Several lineages of *Tympanocryptis* in north-eastern Australian grasslands have remained in question due to a lack of taxonomic resolution based on traditional phylogenetic data and external morphology. Previous work indicated there are potentially three undescribed lineages within this region (Melville et al. 2014). However, limited sampling, a lack of distinguishing morphological characters, and phylogenetic analyses that were unable to rule-out mtDNA introgression, prevented a taxonomic treatment of these lineages. We demonstrate that our integrative taxonomic approach, combining both high-resolution genomic and morphological data, improves confidence in species delimitation within the *Tympanocryptis* genus in north-eastern Australian grasslands.

MATERIALS AND METHODS

Sampling and DNA Extractions

Samples from the three target lineages (Lineage A, B, and C) and closely related taxa from the Great Artesian Basin (GAB) species group (*T. tetraporophora*, *T. condaminensis*, *T. wilsoni*, and *T. pentalineata*) were included in our study. These lineages were originally identified as putative species that needed further sampling in Melville et al. (2014). Our study collected samples throughout their known ranges and across suitable habitats (Fig. 1), with additional samples from Museums Victoria, Queensland Museum, and Western Australia Museum included for species where available.

Genomic DNA was extracted from 348 tail tissue or liver samples using the Qiagen Blood & Tissue Kit (Qiagen, Hilden, Germany) as per manufacturer guidelines, for use in phylogenetic and/or phylogenomic analysis. GenBank data from previously sequenced samples were also incorporated into phylogenetic analyses. At least one sample from all other currently described *Tympanocryptis* species was included to allow
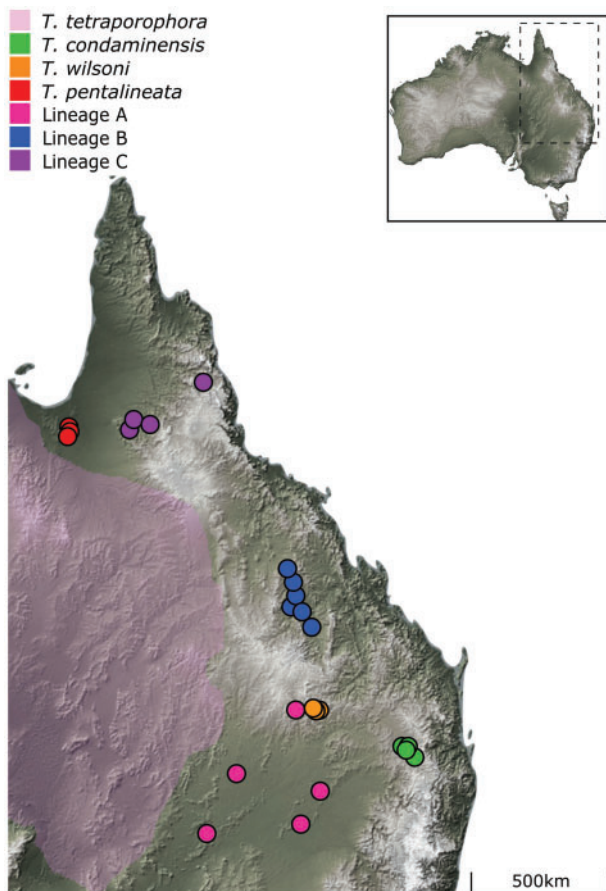
FIGURE 1. Map of sampling sites across the known distribution of north-eastern Australian earless dragon species, including *T. pentalineata*, *T. condaminensis*, *T. wilsoni*, *T. tetraporophora* (distribution shown here as shaded area), and the three target *Tympanocryptis* lineages (A, B, and C).

Phylogeography, Laboratory Protocols and Data Analysis

The mitochondrial gene ND2 and nuclear gene RAG1 were amplified using the primers (Metf.1, COIr.aga, JRAG1f.1, and JRAG1r.13) and protocols described in Shoo et al. (2008). Negative controls were used in each PCR run. Amplification products were visualized on a 1.2% agarose gel with Sybr SAFE (Invitrogen, CA, USA), then purified using ExoSAP-IT (Thermo Fisher, CA, USA) as per manufacturer guidelines, and sent to Macrogen (Seoul, South Korea) for sequencing. Sequence chromatograms were edited and aligned separately in Geneious 6.1.8 (Biomatters, Auckland, New Zealand).

Pairwise uncorrected genetic distances for the ND2 alignment were calculated in Mega7 (Kumar et al. 2016), with the codon frame set as the 3rd nucleotide position. ND2 and RAG1 were each found to follow the GTR+I+G model of substitution with no partitioning schemes using the corrected Akaike Information Criterion (AIC) on PartitionFinder2 on the CIPRES Science Gateway (Miller et al. 2010; Lanfear et al. 2017). RaxML analyses (Stamatakis 2014) for ND2 and RAG1 were performed on XSEDE on the CIPRES Science Gateway using the GTR+G model of substitution (as using the proportion of invariable sites estimate in RaxML is strongly discouraged by the software developers), with 1000 nonparametric bootstraps. Bayesian analyses for ND2 and RAG1 were performed using MrBayes (Huelsenbeck and Ronquist 2001) on the CIPRES Science Gateway, with two runs of four independent MCMC chains (each 50,000,000 generations long, sampled every 1000 generations), under a GTR+I+G model with flat priors. Tracer v1.6 (Rambaut et al. 2014) was used to check for stationarity and convergence of the chain outputs. The trees were subject to a 25% burn-in in MrBayes, summarized and posterior probabilities obtained.

us to determine the phylogenetic relationships within the genus *Tympanocryptis*, and *Amphibolurus muricatus*, *Rankinia diemensis, and Pogona vitticeps* were used as outgroups. Genomic sequencing was undertaken for all available samples from the three target species and GAB species group that met quality control thresholds, and a subset of these individuals were used for geometric morphometric analyses, chosen from populations spanning the geographic range of each species to ensure full representation. Two to three specimens of each sex for each species were used to account for any effect of sex, and only adult specimens were used to remove any effect of ontogeny. Locality data, Museum numbers and GenBank accession numbers of all samples utilized in phylogenetic, phylogenomic, and morphometric analyses are listed in Supplementary Appendix S1 (available on Dryad at http://dx.doi.org/10.5061/dryad.d18gd26). Data files used phylogenetic, phylogenomic, and geometric morphometric analyses available online on Figshare: https://melbourne.figshare.com/s/b569d8264ad4e22d471b.

Phylogenomics Protocols and Data Analysis

The DNA concentration of each extraction sample was quantified using a QIAxpert microfluidic spectrophotometer (Qiagen, Hilden, Germany), and adjusted to 30–100 ng/µL (required for DArTseq arrays). About 15 µL volumes were sent to Diversity Arrays Technology (Canberra, Australia) for digestion using genus-specific restriction enzymes, ligation, amplification and sequencing on an Illumina HiSeq2500 (CA, USA), in a genome complexity reduction method optimized for *Tympanocryptis* species (see Melville et al. 2017 for a detailed description). The genome sequence of the related *Pogona vitticeps* was used as the reference alignment (Georges et al. 2015). The preliminary pipeline applied filters to ensure quality and reproducibility of markers, and a secondary pipeline using DArTseq proprietary calling algorithms scored the genotypes of polymorphic loci across all individuals. The loci were combined into a matrix of SNP genotypes for individuals, with integers representing genotype states compared to the

reference; homozygous; heterozygous; and alternate homozygous.

SNP data were imported into R v3.3.3 (R Core Team 2015) and metadata (genetic lineage, population, sampling locality) assigned with the R package "dartR" (Gruber et al. 2017). The "dartR" package was used to filter the data for all subsequent analyses under several parameters; callrate by individual >0.95, callrate by locus >0.95, monomorphic loci = 0, and reproducibility = 1. Principle coordinates analyses (PCoA) were run using dartR, and the "faststructure" data recoding function was used to generate the files required for analysis by fastSTRUCTURE (Raj et al. 2014). Plink (Purcell et al. 2007) was first used to test for the number of clusters (K), which was subsequently used as the clustering parameter for fastSTRUCTURE analysis. We used the dartR "fasta" function with Method 3 (SNPs are converted to base pairs with heterozygous loci replaced by standard ambiguity codes) to generate a single concatenated sequence for each individual across all loci. Invariant sites were removed using Mesquite (Maddison and Maddison 2009). A Lewis-type ascertainment bias correction was applied to a RaxML analysis of these sequences with 1000 nonparametric bootstraps on XSEDE on CIPRES. The AICc on jModelTest (Posada 2008) on CIPRES indicated a GTR+I+G model of substitution, although GTR+G was used for the RaxML analysis (again, as the use of the proportion of invariable sites estimate is not recommended in RaxML). Pairwise F_{ST} values were calculated using the R package "StAMPP," with 100 bootstraps (Pembleton et al. 2013).

Geometric Morphometric Protocols and Data Analysis

The head of each specimen was scanned using an 180kV nanofocus tube in a Phoenix Nanotom M (GE Measurement & Control, MA, USA) equipped with a tungsten target for 600 projections at 55 kV, 400 μA for 500 ms. The final voxel size was 15 μm. Volumetric reconstructions of the skulls were generated by datos|x-reconstruction software (GE Sensing & Inspection Technologies GmbH, Wunstorf, Germany) and three-dimensional surface models of crania were prepared in VGStudio Max2.1 (Volume Graphics, Heidelberg, Germany). Forty-nine landmarks were chosen to form a holistic representation of overall cranial shape, and were placed across the cranial surface in Landmark Editor v3.6 (Institute of Data Analysis and Visualisation, UC Davis, USA; Fig. 2). Three-dimensional landmark coordinates were exported to MorphoJ (Klingenberg 2011) and subject to a Generalized Procrustes fit to align and orient the points and standardize for size relative to their centroid.

The resulting Procrustes coordinates were used for subsequent analyses in the R v3.3.3 package "geomorph" (Adams and Otárola-Castillo 2013), where statistical tests of significance were subject to 10,000 iterations under a randomized residual permutation procedure.
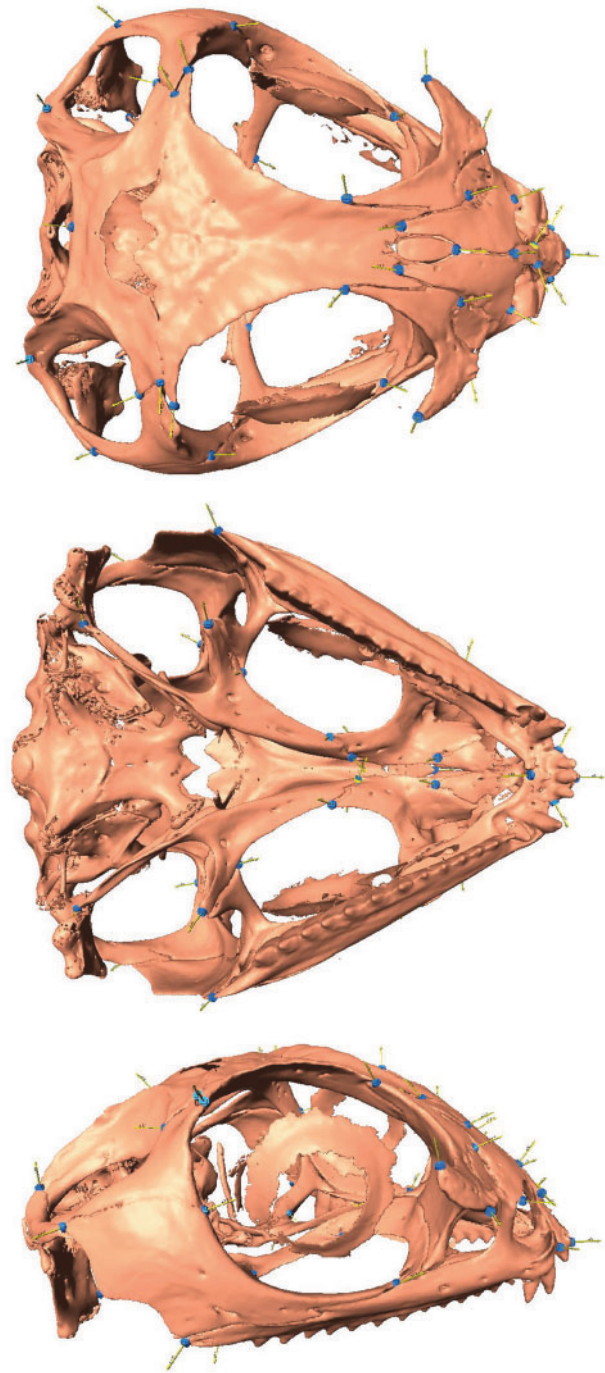

FIGURE 2. Locations of 49 landmarks placed on the cranial 3D models, shown on *Tympanocryptis pentalineata* (NMVD74073) in dorsal, ventral, and lateral view.

A Procrustes analysis of variance (ANOVA) was used to test the effects of sex, log-transformed centroid size, and genomic lineages on cranial shape. For significant lineage effects, tests of pairwise differences based on the Procrustes distances between least-squares means were also performed for the defined groups. A principal component analysis (PCA) was conducted on

the covariance matrix of the Procrustes coordinates in MorphoJ, and shape changes along the first two PC axes were assessed to determine which variables contributed the most to morphological variation among specimens. The negative and positive extremes of each PC axis were illustrated by wireframe graphs connecting the cranial landmarks, shown against a wireframe of the average cranial shape for the entire data set.

SNP data for all scanned specimens (filtered to 10,019 polymorphic loci and converted to sequences, as per methods described previously) were used in a RaxML analysis on XSEDE on CIPRES. A Lewis-type ascertainment bias correction was applied with 1000 nonparametric bootstraps, and a GTR+G model of substitution was used as indicated by the AICc on jModelTest on CIPRES. This genomic phylogeny was then projected into the PCA morphospace to visualize evolutionary relationships in relation to cranial shape. The multivariate K-statistic K_{mult} (Adams 2014a, 2014b) was also used to estimate the strength of phylogenetic signal in cranial shape based on genomic relationships.

RESULTS

Phylogenetic Relationships

There was strong support for the independent evolutionary history of each of the target Lineages A, B, and C based on inferences from the mtDNA ND2 phylogeny (Fig. 3a,b). Each clade was supported as monophyletic, with posterior probabilities and bootstrap branch support values over 0.95/95. However, the evolutionary relationships between major clades were not as highly supported. Within the GAB species group, including *T. condaminensis, T. wilsoni,* and *T. pentalineata,* Lineage A was supported as the sister taxon to the broadly distributed *T. tetraporophora.* Lineages B and C were resolved as sister species, forming a weakly supported clade along the great dividing range (GDR), which was sister to the GAB species group. These GDR lineages were deeply divergent, with long branches, substantial genetic structure within each lineage and mtDNA pairwise uncorrected genetic distances of >10% (Table 1). There was between 4% and 7% uncorrected genetic distances between lineages within the GAB

species group, with 4–6.7% between Lineage A and the other lineages within the GAB clade.

Phylogenetic relationships between clades in the nuclear RAG1 phylogeny were not well supported. Of the undescribed lineages, Lineage A was not supported as monophyletic. The topology of this RAG1 tree differed to that of the mtDNA tree (Fig. 3c). Notably, Lineage A was nested within the *T. tetraporophora,* forming the Eyre-Darling Basin group, along with *T. condaminensis* and *T. wilsoni.* In addition, *T. pentalineata* was the sister lineage to the Eyre-Darling Basin species group. Lastly, the *T. lineata–T. pinguicolla–T. houstoni* species group was recovered as a sister clade to Lineage C.

Based on results from both the mtDNA and RAG1 phylogenies, samples were selected for inclusion in phylogenomics, selecting all from the three target species and GAB species group that met quality control thresholds ($N = 238$).

Phylogenomics

The DArTseq low-density assay produced 120,931 loci across 238 samples. After filtering the full data set for SNP call rate, individual call rate, monomorphs, and reproducibility, 8783 loci across 231 individuals were used for the PCoA, pairwise F_{ST}, and fast-STRUCTURE analyses. All pairwise F_{ST} results were highly significant ($P < 0.001$) with very high levels of genomic fixation, ranging from 0.665 to 0.944 between species (Table 1). There was clear clustering of each molecular lineage in the fastSTRUCTURE plot (Fig. 3d) and distinct grouping in the PCoA (Fig. 4a), indicating the evolutionary independence of each lineage. Very few samples registered any detectable genomic signal discordance (genomic contributions from another lineage), and of these, only one sample had greater than 5% genomic signal discordance (one individual from Lineage C with 11% genomic contribution from *T. pentalineata*).

Principle coordinates one and two in a PCoA of the 8783 loci across 231 individuals accounted for over 66.5% of the genomic variation. The Eyre-Darling Basin species (*T. tetraporophora, T condaminensis, T. wilsoni,* and *Lineage* A) were closely grouped in the PCoA (Fig. 4a), prompting a secondary analysis of just these four lineages. After filtering the data, 39,062 SNP loci across 111 individuals were used for a PCoA of the Eyre-Darling Basin species (Fig. 4b), with 71.9% of the variation explained by PCo1 and PCo2. With greater resolution from additional loci, this second PCoA (Fig. 4b) supports the strong independent genomic identity of each of these lineages, which was swamped in the original PCoA (Fig. 4a) because of the significant genomic distance between the Eyre-Darling Basin group and the other three highly distinct lineages (*T. pentalineata,* Lineage B, and Lineage C).

Phylogenomic analysis of 10,019 polymorphic loci using a corrected Maximum Likelihood approach

TABLE 1. Pairwise F_{ST} values based on 8783 SNP loci (figures above the diagonal) and pairwise uncorrected genetic distance of the mtDNA gene ND2 (figures below the diagonal) for north-eastern Australian *Tympanocryptis* species

	1	2	3	4	5	6	7
1 *T. condaminensis*	–	0.937	0.906	0.723	0.918	0.793	0.892
2 Lineage B	0.096	–	0.908	0.922	0.938	0.919	0.944
3 Lineage C	0.115	0.135	–	0.872	0.892	0.847	0.916
4 Lineage A	0.040	0.106	0.121	–	0.878	0.665	0.842
5 *T. pentalineata*	0.043	0.106	0.120	0.067	–	0.865	0.938
6 *T. tetraporophora*	0.042	0.108	0.112	0.055	0.060	–	0.832
7 *T. wilsoni*	0.048	0.102	0.096	0.061	0.070	0.058	–

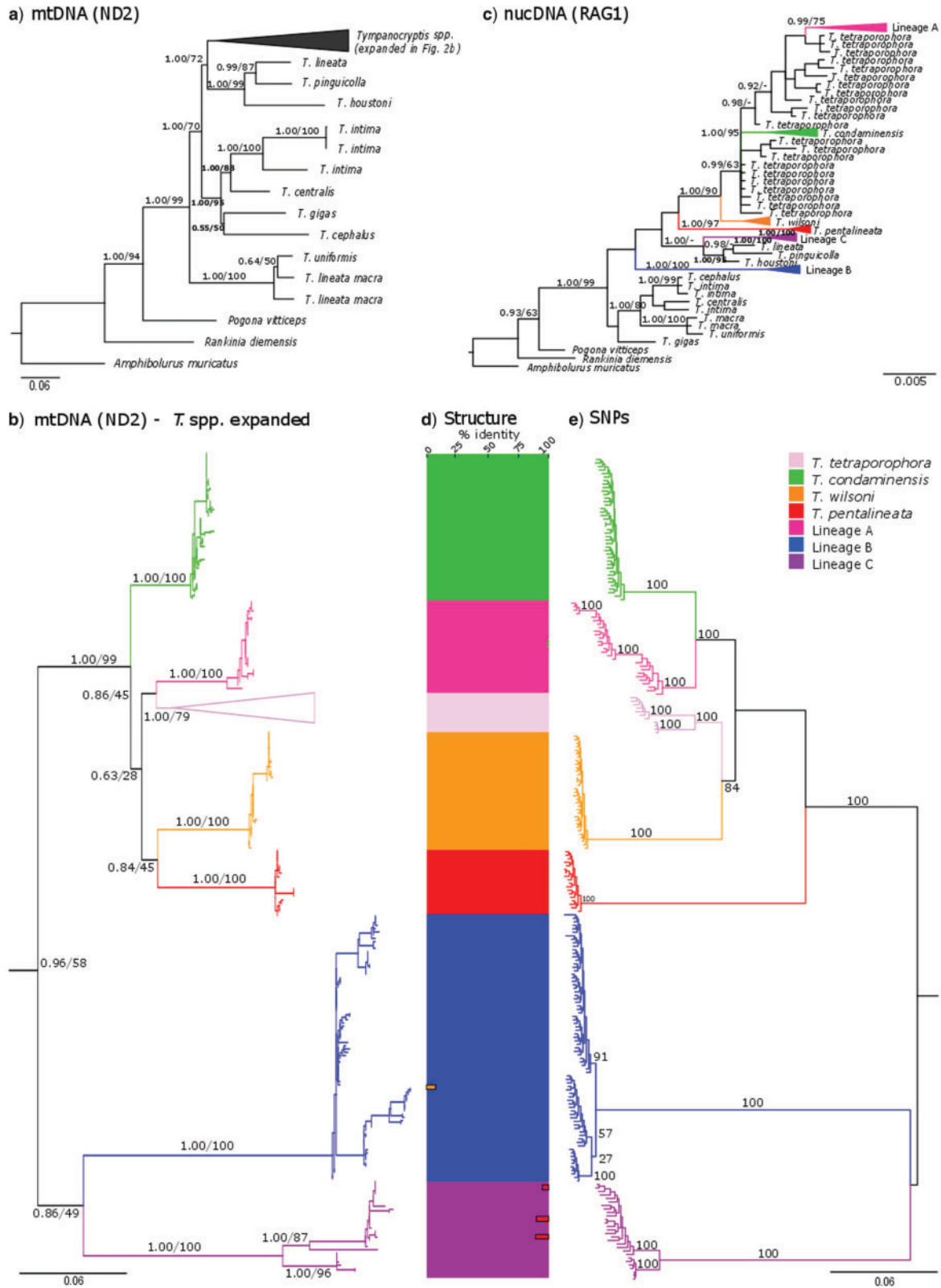Note: All F_{ST} values were highly significant ($P < 0.001$).

FIGURE 3.   Phylogenetic and phylogenomic relationships of earless dragons. a) Phylogeny of *Tympanocryptis* spp. (with north-eastern Australian lineages collapsed) from combined Bayesian and Maximum Likelihood analyses of the mtDNA gene ND2. b) Expanded view of the collapsed north-eastern Australian lineages (*T. pentalineata, T. condaminensis, T. wilsoni, T. tetraporophora*, and Lineages A, B, and C). c) Phylogeny of *Tympanocryptis* spp. including north-eastern Australian target species from combined Bayesian and Maximum Likelihood analyses of the nuclear gene RAG1. d) fastSTRUCTURE plot of target species genomic identity based on 8783 SNP loci and *K* = 7, with each individual represented by a horizontal bar colored by lineage. e) SNP phylogeny of target species from a corrected Maximum Likelihood analysis of 10,019 polymorphic loci. Phylogeny posterior probabilities and bootstrap support values are shown on nodes as PP/BS. Where Maximum Likelihood topology was not analogous with the Bayesian phylogeny nodes are shown as PP/–. Bootstrap values are given in the Maximum Likelihood-only SNP phylogeny. Scale bars indicate the number of nucleotide substitutions per site.
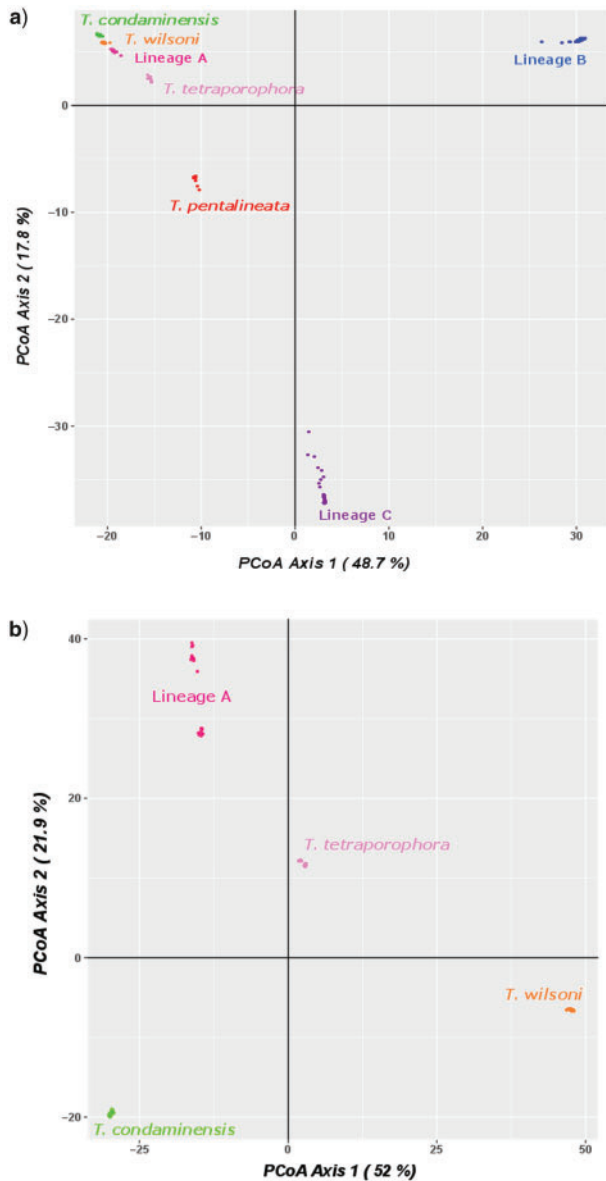
FIGURE 4.   Principle coordinates analysis of (a) 8783 SNP loci for all north-eastern Australian *Tympanocryptis* species (*T. pentalineata, T. condaminensis, T. wilsoni, T. tetraporophora*, and Lineages A, B, and C) and (b) 39,062 SNP loci for the four Eyre-Darling Basin species (*T. condaminensis, T. wilsoni, T. tetraporophora*, and Lineage A).

provided strong support for the independent evolution of each lineage (Fig. 3e). The monophyly of each species and Lineage (A, B, and C) are highly supported and most sister species relationships are also supported with bootstrap values of 100%, except for between *T. tetraporophora* and *T. wilsoni* (bootstrap support = 84%). The topology of the GAB clade in the SNP phylogeny differed slightly to that in the mtDNA phylogeny, with *T. pentalineata* as the most basal lineage, *T. wilsoni* and *T. tetraporophora* supported as sister species, and Species A supported as the sister lineage to *T. condaminensis*.

Geometric Morphometrics

A subset of individuals included in the phylogenomic analyses was used for GM (N = 34), chosen from populations spanning the geographic range of each species/lineage, with 2–3 specimens of each sex per lineage. There was a significant but weak effect of log-transformed centroid size on cranial shape (R^2 = 0.0871, P = 0.0011), and a weak but nonsignificant effect of sex (R^2 = 0.0482, P = 0.0639). Cranial shape variation was strongly correlated with species identity (R^2 = 0.438, P < 0.0001), with all species pairs showing significant differences except *T. wilsoni* and Lineage A (Table 2).

The PCA of cranial shape revealed distinct clustering of individuals in each species concordant with the phylogenomic topology, with little overlap between genomic lineages except for the above-noted pair (Fig. 5a). Together PC1 and PC2 accounted for 36% of the total shape variation, with PC1 related to width and depth of the cranium, and PC2 describing variation in the angle of the snout. Subsequent PC axes accounted for <9% of the total variation each. CT images of example skulls together with wireframe graphs of the average change in landmark positions for each lineage illustrate morphological variation in *Tympanocryptis* (Fig. 5b). Individuals from Lineage B and C possess a slightly narrower, deeper skull with a longer snout, while those from *T. pentalineata*, Lineage A, and *T. wilsoni* exhibit wider, shallower skulls with shorter snouts. Shape change along the second PC showed *T. pentalineata* and Lineage C individuals possessing more blunt snouts (positive PC2), while Lineage B and *T. wilsoni* displayed more tapered or elongated features (negative PC2). Overall, there was a highly significant but weak phylogenetic signal (K_{mult} = 0.05, P = 0.0001) in the cranial morphology of these species.

DISCUSSION

Integrative Taxonomic Approach for Cryptic Species Delimitation

Integrative taxonomy is now a widely used approach for species delimitation (Dayrat 2005; Padial et al. 2010; Schlick-Steiner et al. 2010). Our review of 29 recent species delimitation studies using "integrative taxonomy" for cryptic complexes (Table 3), shows the majority used external morphology and traditional phylogenetics combined with multivariate statistics to identify differences between clades. There are varying levels of effectiveness in using this simple form of species delimitation, with some studies successfully delimiting many species (Ceccarelli et al. 2012; Grismer et al. 2013), and other studies unable to confidently or consistently distinguish species (Wiens and Penkrot 2002; Satler et al. 2013). Other more novel methods of delimiting species, including bioacoustics (Meegaskumbura et al. 2002; Padial and De la Riva 2009), behavioral ecology (Tan et al. 2010), chemical compound

TABLE 2.   Pairwise distance matrix of cranial shape variation between north-eastern Australian *Tympanocryptis* species

	T. condaminensis	*T. pentalineata*	Lineage A	Lineage B	Lineage C	*T. wilsoni*
T. condaminensis	—	0.0464	0.0442	0.0424	0.0477	0.0448
T. pentalineata	0.0122	—	0.0454	0.0567	0.0621	0.0444
Lineage A	0.0203	0.0029	—	0.0507	0.0599	0.0355
Lineage B	0.0348	0.0001	0.0007	—	0.0465	0.0426
Lineage C	0.0069	0.0001	0.0001	0.0019	—	0.0610
T. wilsoni	0.0163	0.0041	0.0720	0.0088	0.0001	—

Note: Figures above the diagonal indicate the pairwise least-squares mean distances, supported by *P*-values listed below.

analysis (Heethoff et al. 2011; Leavitt et al. 2011), and ecological niche modeling (Rissler and Apodaca 2007; Wielstra and Arntzen 2014) were sometimes incorporated as additional lines of evidence to traditional morphology and genetic data. There has also been increasing use of phylogenetic or phylogenomic modeling approaches, with some studies including phenotypic trait data in Bayesian multispecies coalescent models (Solís-Lemus et al. 2015; Pyron et al. 2016; Singhal et al. 2018).

Taxonomic studies using an integrative taxonomic framework with genomic data are still few (Table 3), but rapidly increasing. The high numbers of loci gained from using genomic approaches can offer much-needed resolution for cryptic taxa or species complexes (Padial et al. 2010; Pyron et al. 2016; Raupach et al. 2016; Singhal et al. 2018), with multiple applicable genomic techniques (e.g., RADseq, exon capture, whole-genome sequencing, transcriptomics and many more [Lemmon and Lemmon 2013; Andrews and Luikart 2014]). Pyron et al. (2016) used an anchored-loci NGS technique isolating 322 loci, (totaling 227,911 bp), and combined these genomic data with morphological trait data in the common Bayesian multispecies coalescent model iBPP (Solís-Lemus et al. 2015). In contrast, Leaché et al. (2014) did not incorporate morphological data, but used 1087 SNP loci from double-digest RADseq (Peterson et al. 2012), and built on the Bayes factor delimitation (BFD) approach (Grummer et al. 2014) to produce a genomic-based version (BFD*) of the model. Both of these phylogenomic modeling approaches were successful in delimiting species, with Leaché et al. (2014) finding the BFD* method to be consistently effective even with low sample sizes.

The use of CT imaging in morphological, paleontological, and taxonomic studies is also becoming more frequent (Sobral et al. 2012; Stoev et al. 2013; Akkari et al. 2015; Hipsley and Sherratt 2019) but has not, until now, been integrated with genomic data for species delimitation. There are many advantages of using CT for morphometric analyses, including data accuracy through multidimensional landmarking of morphological characters, nondestructive sampling of museum specimens, and additional information regarding evolutionary history of taxa that may only be seen through internal anatomical variation (Spoor et al. 1994; Faulwetter et al. 2013; Fernández et al. 2014). Comparative evolutionary techniques now also allow the integration of phylogenomic data into geometric morphometric analyses, which can provide greater taxonomic resolution than that gained from traditional morphological measurements (Klages et al. 2013; Stoev et al. 2013). This comparative approach has broad applications for assessing species delimitation of externally cryptic taxa, by revealing hidden osteological variation (Klages et al. 2013; Fernández et al. 2014; Prötzel et al. 2018).

Many taxonomic studies using micro-CT have been limited to using only a single specimen (or few specimens) per lineage, which may not reflect the geographic or sex-based variation within each taxonomic unit, and limits the use of comparative analytical approaches. We resolve this limitation with a step-down approach for selection of multiple specimens to be CT scanned, allowing us to capture any sex-based and phylogeographic variation within and between genomic lineages. This representation of variation as part of a whole-evidence approach offers greater confidence in delimitation. Our step-down approach (summarized in Fig. 6) provides a novel species delimitation method that would be broadly applicable across morphologically cryptic groups.

North-Eastern Australian Tympanocryptis Species Delimitation

By integrating phylogeographic, phylogenomic, and geometric morphometric data, our study provides additional taxonomic support for currently described *Tympanocryptis* species (*T. tetraporophora*, *T. condaminensis*, *T. wilsoni*, and *T. pentalineata*) and strong evidence of three undescribed species (Lineages A, B, and C). We found geographically associated relationships between evolutionary lineages, with two broad geographic groups: 1) the GDR Lineages B and C; and 2) the GAB lineages *T. tetraporophora*, *T condaminensis*, *T. wilsoni*, Lineage A, and *T. pentalineata*. A subset of the GAB was also consistently recovered in nuclear and genomic analyses, comprising the Eyre-Darling Basin species group (*T. tetraporophora*, *T condaminensis*, *T. wilsoni*, and Lineage A).

The high pairwise F_{ST} values, based on SNP data, of the taxa in this study indicate the evolutionary stationarity and fixation of each mtDNA lineage (Wright 1978). Lineage A and *T. tetraporophora* had the lowest pairwise F_{ST} value of 0.665, concordant with the clustering configuration in the Eyre-Darling Basin PCoA (Fig. 4b), although an F_{ST} of 0.665 is still indicative of little recent gene exchange between
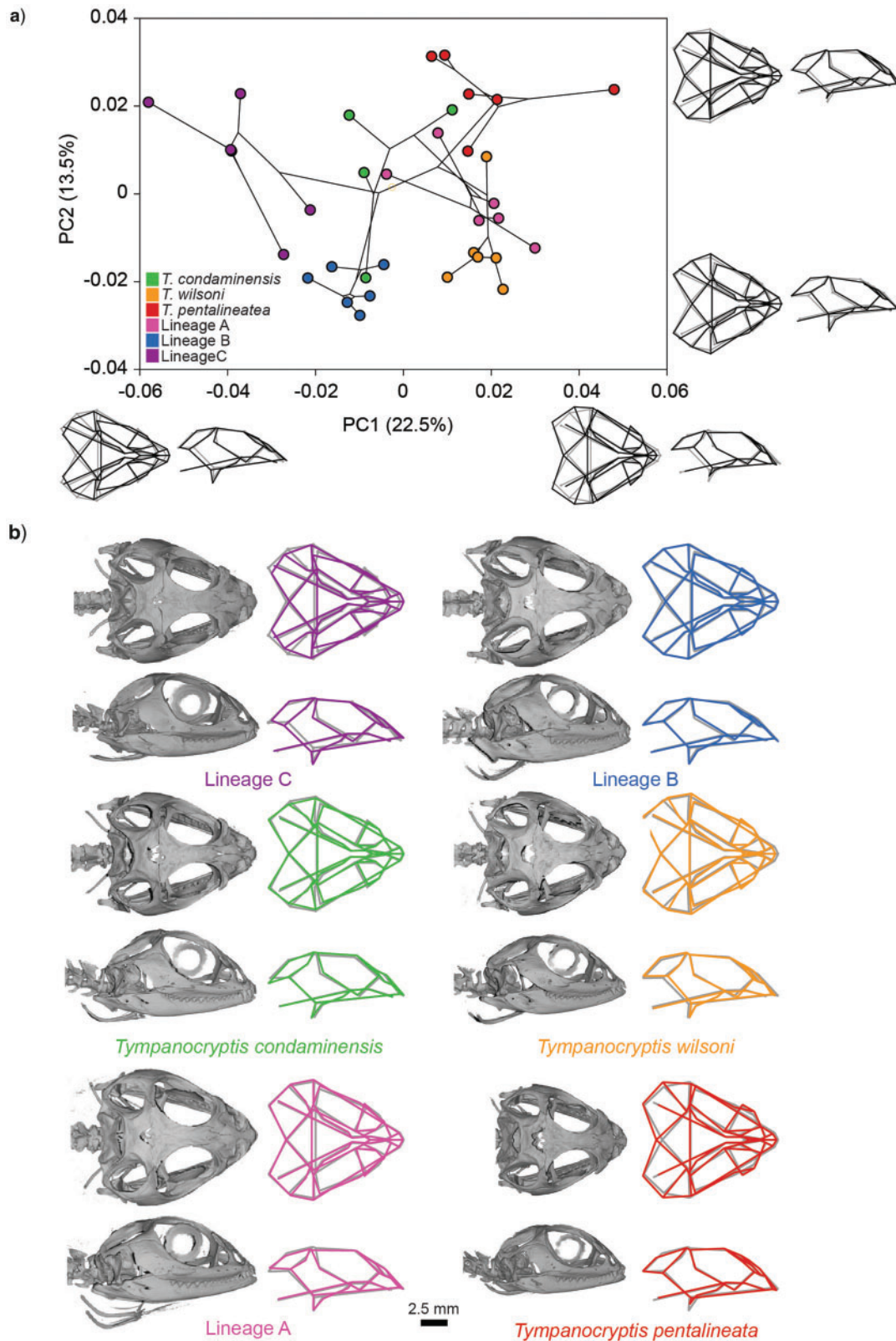
FIGURE 5.   Cranial morphology of north-eastern Australian *Tympanocryptis* species. a) PCA plot of cranial shape variation based on the landmark data, with the corrected Maximum Likelihood phylogeny using 8860 polymorphic SNP loci projected into morphospace. Wireframe graphs connecting cranial landmarks show the extreme shape change at the ends of each PC axis in black, compared to the average cranial shape for the full data set in gray. b) Representative skulls from each lineage chosen from near the center of their morphospace distribution, next to colored wireframes of the average shape for that lineage compared with the overall average in gray. Specimens are arranged in order of their PC1 scores, from negative to positive.

TABLE 3. A review of the methods used in 29 recent species delimitation studies, including those involving cryptic species with the stated use of "integrative taxonomy"

Integrative approaches used	Examples of studies
Phylogenetics and ecological niche modeling	Rissler and Apodaca (2007), Wielstra and Arntzen (2014)
Phylogenetics and multivariate statistics of external morphology including	Wiens and Penkrot (2002), Wagner et al. (2011), Ceccarelli et al. (2012), Grismer et al. (2013), Satler et al. (2013), Shirley et al. (2014), Papakostas et al. (2016)
CT imagery	Pyle et al. (2008), Klages et al. (2013), Stoev et al. (2013), Prötzel et al. (2018)
Phenotypic chemistry	Heethoff et al. (2011), Leavitt et al. (2011)
Color photometry	McKay et al. (2014)
Other ecology/biology	Meegaskumbura et al. (2002), Hebert et al. (2004), Padial and De la Riva (2009), Tan et al. (2010), Smith et al. (2011)
Modeling of phylogenetic data (Bayesian multispecies coalescent or Bayes factor delimitation) including External morphology	Liu and Pearl (2007), Leaché and Fujita (2010), Yang and Rannala (2010)
	Drummond et al. (2012), Solís-Lemus et al. (2015)
Modeling of phylogenomic data (Bayesian multispecies coalescent or Bayes factor delimitation) including External morphology	Leaché et al. (2014)
	Pyron et al. (2016); Singhal et al. (2018)

Note: Common sets of approaches are grouped, with examples of studies using each combination of integrative techniques.
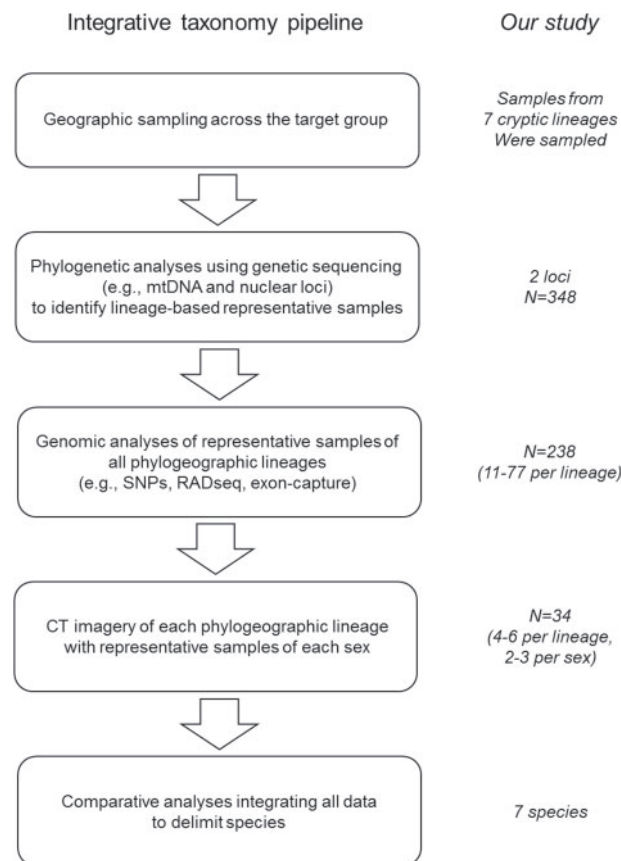

FIGURE 6. The step-down integrative taxonomy workflow used in our study, designed to capture sex-based and geographical variation within each lineage. This whole-evidence approach combines single-gene phylogeographic, genomic and 3D computed tomography (CT) data to provide confidence in delimiting species. We provide details of the data sampling and subsampling using alongside the step-down workflow.

taxa (Hartl and Clark 1997). Each mtDNA lineage was highly supported as monophyletic. In contrast, in the RAG1 phylogeny, a number of lineages remained unresolved, with several incongruences between the topology of this nuclear phylogeny and the mtDNA phylogeny, probably

due to differing evolutionary histories of each gene (Brown et al. 1982; Caccone et al. 2004). The lack of taxonomic resolution that a single nuclear gene often provides is clear in this study, confirming that multilocus approaches are required (Moore 1995; Dayrat 2005; Satler et al. 2013; Papakostas et al. 2016). The resolution achieved by the genome-wide SNP analyses reflects their utility, especially when combined with an initial baseline mtDNA phylogeographic analysis. Our approach provided a robust assessment of evolutionary lineages within north-eastern Australian *Tympanocryptis*. However, we support the recommendation of Coates et al. (2018), that a conservative approach needs to be taken with species delimitation and that basing taxonomic decisions solely on genomic data risks over-splitting species, with population-level structure misconstrued as species-level diversity.

To address such problems, we ensured that sampling in our study was comprehensive enough to observe population-level genomic structure relating to the geographic distribution of lineages. This geographic-based genomic structure was most evident in the target Lineages A, B, and C, as well as the widely distributed *T. tetraporophora.* However, the distance between the sampled populations of *T. tetraporophora* (>1100 km) is far greater than the maximum distribution of populations of each of Lineage A (maximum 275 km), Lineage B (maximum 190 km), and Lineage C (maximum 320 km). This genomic structure within lineages over relatively small geographic space suggests a complex evolutionary history in these regions of north-eastern Australia. This population-level structuring within lineages provides greater confidence that our taxonomic decisions accurately reflect species-level diversity.

In concordance with the phylogeographic and phylogenomic analyses, geometric morphometric analyses found significant evidence of osteological variation among the north-eastern Australian *Tympanocryptis* lineages. Species identity based on cranial morphology was supported by *post hoc* tests identifying significant pairwise differences, revealing phenotypic distinctiveness that had not been identified previously in this morphologically cryptic group (see Melville et al. 2014). However, there was only a weak phylogenetic signal in cranial shape between lineages, indicating that variation in skull shape between these lineages is far less than that expected by their genetic divergence. This result, with deep genetic structure but little morphological divergence, suggests selection pressure or morphological stasis limiting phenotypic divergence in these lizards (Melville et al. 2006; Smith et al. 2011). Although they are allopatric, most of these species inhabit similar habitats (grasslands on cracking soils), and may be subject to convergent selection pressures (Wiens and Rotenberry 1980; Losos 2008; Smith et al. 2011).

Prior to this study, the taxonomy of these north-eastern Australian earless dragons had remained unresolved.

Our integration of traditional phylogeographic data with genomics and GM provides a robust whole-evidence approach to species delimitation in this cryptic group of lizards. These data should provide confidence in future taxonomic work undertaken on this group.

CONCLUSION

Integrative taxonomic studies, with the goal of species delimitation in cryptic complexes, have progressed significantly over the last decade, largely due to developments in molecular techniques with the use of genomics and advanced analytical approaches. At the same time, the types of phenotypic data collected for biological studies have also evolved from largely linear, size-based metrics to high-dimensional multivariate landmark data. However, measurements of external morphology using microscopes, calipers or rulers remain standard practice for most cryptic species treatments, which often lack the resolution required to distinguish between cryptic lineages. Here, we demonstrated new approaches that provide high-resolution morphological data which, when combined with phylogenomics, allow accurate classification of cryptic species using three-dimensional landmarks and geometric morphometric analyses. Although this presents an exciting direction for future integrative taxonomic work in the genomic age, we stress that caution is needed with these powerful techniques against the risk of over-splitting species. We recommend adequate sampling, both across geographic space and within lineages, to encompass the range of intraspecific variation. Such an approach will allow quantification of within versus between lineage variations to allow informed decision-making in these cryptic species complexes.

SUPPLEMENTARY MATERIAL

Data available from the Dryad Digital Repository: http://dx.doi.org/10.5061/dryad.d18gd26.

P. and P. Halford, R. Hobson, S. Wilson, P. Couper, and A. Amey for help in the field collection of earless dragon tissues and specimens. They would also like to thank M. Haines, B. Hamdan and S. Kazi for their assistance with analyses.

Data Accessibility

- Raw data files, including those used for phylogeography (mtDNA & RAG1), genomics (SNPs), and GM (CT scans and landmark files), are available on Figshare: https://melbourne.figshare.com/s/b569d8264ad4e22d471b.

- Specimens used for genomics and CT scanning are all held in museum collections in Australia; accession numbers available in Supplementary Appendix S1 available on Dryad.

References

Abdelaziz M., Lorite J., Muñoz-Pajares A.J., Herrador M.B., Perfectti F., Gómez J.M. 2011. Using complementary techniques to distinguish cryptic species: a new Erysimum (Brassicaceae) species from North Africa. Am. J. Bot. 98:1049–1060.

Adams D.C. 2014a. A generalized K statistic for estimating phylogenetic signal from shape and other high-dimensional multivariate data. Syst. Biol. 63:685–697.

Adams D.C. 2014b. A method for assessing phylogenetic least squares models for shape and other high-dimensional multivariate data. Evolution. 68:2675–2688.

Adams D.C., Otárola-Castillo E. 2013. Geomorph: an R package for the collection and analysis of geometric morphometric shape data. Methods Ecol. Evol. 4:393–399.

Adams D.C., Otárola-Castillo E., Paradis E. 2013. Geomorph: an R package for the collection and analysis of geometric morphometric shape data. Methods Ecol. Evol. 4:393–399.

Adams D.C., Rohlf F.J., Slice D.E. 2013. A field comes of age: geometric morphometrics in the 21st century. Hystrix. 24:7–14.

Akkari N., Enghoff H., Metscher B.D. 2015. A new dimension in documenting new species: high-detail imaging for myriapod taxonomy and first 3D cybertype of a new millipede species (Diplopoda, Julida, Julidae). PLoS One. 10:e0135243.

Andrews K.R., Luikart G. 2014. Recent novel approaches for population genomics data analysis. Mol. Ecol. 23:1661–1667.

Bickford D., Lohman D.J., Sodhi N.S., Ng P.K., Meier R., Winker K., Ingram K.K., Das I. 2007. Cryptic species as a window on diversity and conservation. Trends Ecol. Evol. 22:148–155.

Brown W.M., Prager E.M., Wang A., Wilson A.C. 1982. Mitochondrial DNA sequences of primates: tempo and mode of evolution. J. Mol. Evol. 18:225–239.

Bruna E.M., Fisher R.N., Case T.J. 1996. Morphological and genetic evolution appear decoupled in Pacific skinks (Squamata: Scincidae: Emoia). Proc. R. Soc. Lond. B. 263:681–688.

Caccone A., Gentile G., Burns C.E., Sezzi E., Bergman W., Ruelle M., Saltonstall K., Powell J.R. 2004. Extreme difference in rate of mitochondrial and nuclear DNA evolution in a large ectotherm, Galapagos tortoises. Mol. Phylogenet. Evol. 31:794–798.

Caro A., Gomez-Moliner B.J., Madeira M.J. 2019. Integrating multilocus DNA data and 3D geometric morphometrics to elucidate species boundaries in the case of Pyrenaearia (Pulmonata: Hygromiidae). Mol. Phylogenet. Evol. 132:194–206.

Ceccarelli F.S., Sharkey M.J., Zaldívar-Riverón A. 2012. Species identification in the taxonomically neglected, highly diverse, neotropical parasitoid wasp genus Notiospathius (Braconidae: Doryctinae) based on an integrative molecular and morphological approach. Mol. Phylogenet. Evol. 62:485–495.

Coates D.J., Byrne M., Moritz C. 2018. Genetic diversity and conservation units: dealing with the species-population continuum in the age of genomics. Front. Ecol. Evol. 6:165.

Collyer M.L., Sekora D.J., Adams D.C. 2015. A method for analysis of phenotypic change for phenotypes described by high-dimensional data. Heredity. 115:357–365.

Cruz V.M.V., Kilian A., Dierig D.A. 2013. Development of dart marker platforms and genetic diversity assessment of the U.S. Collection of the new oilseed crop Lesquerella and related species. PLoS One. 8:e64062.

Dayrat B. 2005. Towards integrative taxonomy. Biol. J. Linn. Soc. 85:407–415.

De Salle R., Egan M.G., Siddall M. 2005. The unholy trinity: taxonomy, species delimitation and DNA barcoding. Philos. Trans. R. Soc. Lond. B Biol. Sci. 360:1905–1916.

Doughty P., Kealley L., Shoo L.P., Melville J. 2015. Revision of the Western Australian pebble-mimic dragon species-group (Tympanocryptis cephalus: Reptilia: Agamidae). Zootaxa. 4039:85–117.

Drummond A.J., Suchard M.A., Xie D., Rambaut A. 2012. Bayesian phylogenetics with BEAUTi and the BEAST 1.7. Mol. Phyl. Evol. 29:1969–1973.

Esquerré D., Ramírez-Álvarez D., Pavón-Vázquez C.J., Troncoso-Palacios J., Garín C.F., Keogh J.S., Leaché A.D. 2019. Speciation across mountains: phylogenomics, species delimitation and taxonomy of the Liolaemus leopardinus clade (Squamata, Liolaemidae). Mol. Phyl. Evol. 139:106524.

Faulwetter S., Vasileiadou A., Kouratoras M., Thanos D., Arvanitidis C. 2013. Micro-computed tomography: introducing new dimensions to taxonomy. Zookeys. 263:1–45.

Fernández R., Kvist S., Lenihan J., Giribet G., Ziegler A. 2014. Sine systemate chaos? A versatile tool for earthworm taxonomy: non-destructive imaging of freshly fixed and museum specimens using micro-computed tomography. PLoS One. 9:e96617.

Fišer C., Robinson C.T., Malard F., 2018. Cryptic species as a window into the paradigm shift of the species concept. Molecular Ecology, 27:613–635.

Gabelaia M., Tarkhnishvili D., Adriaens D. 2018. Use of three-dimensional geometric morphometrics for the identification of closely related species of Caucasian rock lizards (Lacertidae: Darevskia). Biol. J. Linn. Soc. 125:709–717.

Georges A., Li Q., Lian J., O'Meally D., Wang Z., Zhang P., Fujita M., Patel H.R., Holleley C.E., Zhou Y., Zhang X., Matsubara K., Waters P., Graves J.A.M., Sarre S.D., Zhang G. 2015. High-coverage sequencing and annotated assembly of the genome of the Australian dragon lizard Pogona vitticeps. Gigascience. 4:45.

Gottscho A.D., Wood D.A., Vandergast A.G., Lemos-Espinal J., Gatesy J., Reeder T.W. 2017. Lineage diversification of fringe-toed lizards (Phrynosomatidae: Uma notata complex) in the Colorado Desert: delimiting species in the presence of gene flow. Mol. Phyl. Evol. 106:103–117.

Grismer L.L., Wood P.L. Jr., Anuar S., Muin M.A., Quah E.S., McGuire J.A., Brown R.M., Van Tri N., Hong Thai P. 2013. Integrative taxonomy uncovers high levels of cryptic species diversity in Hemiphyllodactylus bleeker, 1860 (Squamata: Gekkonidae) and the description of a new species from peninsular Malaysia. Zool. J. Linn. Soc. 169:849–880.

Gruber B., Unmack P.J., Berry O.F., Georges A. 2017. DARTr: an R package to facilitate analysis of SNP data generated from reduced representation genome sequencing. Mol. Ecol. Resour. 18:691–699.

Grummer J.A., Bryson J.R.W., Reeder T.W. 2014. Species delimitation using Bayes factors: simulations and application to the Sceloporus scalaris species group (Squamata: Phrynosomatidae). Syst. Biol. 63:119–133.

Hartl D.L., Clark A.G. 1997. Principles of population genetics. Sunderland, MA: Sinauer Associates.

Hebert P.D.N., Gregory T.R. 2005. The promise of DNA barcoding for taxonomy. Syst. Biol. 54:852–859.

Hebert P.D., Penton E.H., Burns J.M., Janzen D.H., Hallwachs W. 2004. Ten species in one: DNA barcoding reveals cryptic species in the neotropical skipper butterfly Astraptes fulgerator. Proc. Nat. Acad. Sci. USA. 101:14812–14817.

Heethoff M., Laumann M., Weigmann G., Raspotnig G. 2011. Integrative taxonomy: combining morphological, molecular and chemical data for species delineation in the parthenogenetic *Trhypochthonius tectorum* complex (Acari, Oribatida, Trhypochthoniidae). Front. Zool. 8:2.

Hipsley C.A., Sherratt E. 2019. Psychology, not technology, is our biggest challenge to open digital morphology data. Sci. Data. 6:41.

Huelsenbeck J.P., Ronquist F. 2001. Mrbayes: Bayesian inference of phylogenetic trees. Bioinformatics. 17:754–755.

Jaccoud D., Peng K., Feinstein D., Kilian A. 2001. Diversity arrays: a solid state technology for sequence information independent genotyping. Nucleic Acids Res. 29:e25.

Karanovic T., Djurakic M., Eberhard SM. 2016. Cryptic species or inadequate taxonomy? Implementation of 2D geometric morphometrics based on integumental organs as landmarks for delimitation and description of copepod taxa. Syst. Biol. 65:304–327.

Klages J., Glaw F., Köhler J., Müller J., Hipsley C.A., Vences M. 2013. Molecular, morphological and osteological differentiation of a new species of microhylid frog of the genus *Stumpffia* from northwestern Madagascar. Zootaxa. 3717:280–300.

Klingenberg C.P. 2011. MorphoJ: an integrated software package for geometric morphometrics. Mol. Ecol. Resour. 11:353–357.

Kordbacheh A., Wallace R.L., Walsh E.J. 2018. Evidence supporting cryptic species within two sessile microinvertebrates, *Limnias melicerta* and *L. ceratophylli* (Rotifera, Gnesiotrocha). PLoS One. 13:e0205203.

Kumar S., Banks T.W., Cloutier S. 2012. SNP discovery through next-generation sequencing and its applications. Int. J. Plant Genomics. 2012:831460.

Kumar S., Stecher G., Tamura K. 2016. MEGA7: molecular evolutionary genetics analysis version 7.0 for bigger datasets. Mol. Biol. Evol. 33:1870–1874.

Kvist S. 2013. Barcoding in the dark?: a critical view of the sufficiency of zoological DNA barcoding databases and a plea for broader integration of taxonomic knowledge. Mol. Phylogenet. Evol. 69:39–45.

Lanfear R., Frandsen P.B., Wright A.M., Senfeld T., Calcott B. 2017. PartitionFinder 2: new methods for selecting partitioned models of evolution for molecular and morphological phylogenetic analyses. Mol. Biol. Evol. 34:772–773.

Leaché A.D., Fujita M.K. 2010. Bayesian species delimitation in west African forest geckos (*Hemidactylus fasciatus*). Proc. Biol. Sci. 277:3071–3077.

Leaché A.D., Fujita M.K., Minin V.N., Bouckaert R.R. 2014. Species delimitation using genome-wide SNP data. Syst. Biol. 63:534–542.

Leavitt S.D., Johnson L.A., Goward T., Clair L.L.S. 2011. Species delimitation in taxonomically difficult lichen-forming fungi: an example from morphologically and chemically diverse *Xanthoparmelia* (Parmeliaceae) in North America. Mol. Phylogenet. Evol. 60:317–332.

Lemmon E.M., Lemmon A.R. 2013. High-throughput genomic data in systematics and phylogenetics. Annu. Rev. Ecol. Evol. Syst. 44:99–121.

Lipscomb D., Platnick N., Wheeler Q. 2003. The intellectual content of taxonomy: a comment on DNA taxonomy. Trends Ecol. Evol. 18:65–66.

Liu L., Pearl D.K. 2007. Species trees from gene trees: reconstructing Bayesian posterior distributions of a species phylogeny using estimated gene tree distributions. Syst. Biol. 56:504–514.

Losos J.B. 2008. Phylogenetic niche conservatism, phylogenetic signal and the relationship between phylogenetic relatedness and ecological similarity among species. Ecol. Lett. 11:995–1003.

Maddison W.P., Maddison D.R. 2009. Mesquite: a modular system for evolutionary analysis. 2011. See http://mesquiteproject.org.

Mathews L.M., Schubart C.D., Neigel J.E., Felder D.L. 2002. Genetic, ecological, and behavioural divergence between two sibling snapping shrimp species (Crustacea: Decapoda: Alpheus). Mol. Ecol. 11:1427–1437.

McKay B.D., Mays J.H.L., Yao C-T., Wan D., Higuchi H., Nishiumi I. 2014. Incorporating color into integrative taxonomy: analysis of the varied tit (*Sittiparus varius*) complex in east Asia. Syst. Biol. 63:505–517.

Meegaskumbura M., Bossuyt F., Pethiyagoda R., Manamendra-Arachchi K., Bahir M., Milinkovitch M., Schneider C. 2002. Sri Lanka: an amphibian hot spot. Science. 298:379–379.

Melville J., Goebel S., Starr C., Keogh J.S., Austin J.J. 2007. Conservation genetics and species status of an endangered Australian dragon, *Tympanocryptis pinguicolla* (Reptilia: Agamidae). Conserv. Genet. 8:185–195.

Melville J., Haines M.L., Boysen K., Hodkinson L., Date K.L.S., Potvin D.A., Kilian A., Parris K.M. 2017. Identifying hybridization and admixture using SNPs: application of the DArTSeq platform in phylogeographic research on vertebrates. R. Soc. Open Sci. 4:161061.

Melville J., Harmon L.J., Losos J.B. 2006. Intercontinental community convergence of ecology and morphology in desert lizards. Proc. Biol. Sci. 273:557–563.

Melville J., Smith K., Hobson R., Hunjan S., Shoo L. 2014. The role of integrative taxonomy in the conservation management of cryptic species: the taxonomic status of endangered earless dragons (Agamidae: *Tympanocryptis*) in the grasslands of Queensland, Australia. PLoS One. 9:e101847.

Milankov V., Ludoški J., Ståhls G., Stamenković J., Vujić A. 2009. High molecular and phenotypic diversity in the Merodon avidus complex (Diptera, Syrphidae): cryptic speciation in a diverse insect taxon. Zool. J. Linnean. Soc. 155:819–833.

Miller M.A., Pfeiffer W., Schwartz T. 2010. Creating the CIPRES science gateway for inference of large phylogenetic trees. Gateway Computing Environments Workshop (GCE), New Orleans, LA, USA.

Moore W.S. 1995. Inferring phylogenies from mtDNA variation: mitochondrial-gene trees versus nuclear-gene trees. Evolution. 49:718–726.

Morin P.A., Luikart G., Wayne R.K. 2004. SNPs in ecology, evolution and conservation. Trends Ecol. Evol. 19:208–216.

Moritz C., Cicero C. 2004. DNA barcoding: promise and pitfalls. PLoS Biol. 2:e354.

Oliver P., Hugall A., Adams M., Cooper S.J., Hutchinson M. 2007. Genetic elucidation of cryptic and ancient diversity in a group of Australian diplodactyline geckos: the Diplodactylus vittatus complex. *Molecular Phylogenetics and Evolution*, 44:77–88.

Padial J.M., De la Riva I. 2009. Integrative taxonomy reveals cryptic Amazonian species of *Pristimantis* (Anura: Strabomantidae). Zool. J. Linn. Soc. 155:97–122.

Padial J.M., Miralles A., De la Riva I., Vences M. 2010. The integrative future of taxonomy. Front. Zool. 7:16.

Papakostas S., Michaloudi E., Proios K., Brehm M., Verhage L., Rota J., Peña C., Stamou G., Pritchard V.L., Fontaneto D., Declerck S.A.J. 2016. Integrative taxonomy recognizes evolutionary units despite widespread mitonuclear discordance: evidence from a rotifer cryptic species complex. Syst. Biol. 65:508–524.

Pembleton L.W., Cogan N.O., Forster J.W. 2013. StAMPP: an R package for calculation of genetic differentiation and structure of mixed-ploidy level populations. Mol. Ecol. Resour. 13:946–952.

Peterson B.K., Weber J.N., Kay E.H., Fisher H.S., Hoekstra H.E. 2012. Double digest RADseq: an inexpensive method for de novo SNP discovery and genotyping in model and non-model species. PLoS One. 7:e37135.

Posada D. 2008. Jmodeltest: phylogenetic model averaging. Mol. Biol. Evol. 25:1253–1256.

Prötzel D., Vences M., Hawlitschek O., Scherz M.D., Ratsoavina F.M., Glaw F. 2018. Endangered beauties: micro-CT cranial osteology, molecular genetics and external morphology reveal three new species of chameleons in the *Calumma boettgeri* complex (Squamata: Chamaeleonidae). Zool. J. Linn. Soc. 184:471–498.

Purcell S., Neale B., Todd-Brown K., Thomas L., Ferreira M.A., Bender D., Maller J., Sklar P., de Bakker P.I., Daly M.J., Sham P.C. 2007. plink: a tool set for whole-genome association and population-based linkage analyses. Am. J. Hum. Genet. 81:559–575.

Pyle R.L., Earle J.L., Greene B.D. 2008. Five new species of the damselfish genus *Chromis* (Perciformes: Labroidei: Pomacentridae) from deep coral reefs in the tropical western Pacific. Zootaxa. 1671:3–31.

Pyron R.A., Hsieh F.W., Lemmon A.R., Lemmon E.M., Hendry C.R. 2016. Integrating phylogenomic and morphological data to assess candidate species-delimitation models in brown and red-bellied snakes (*Storeria*). Zool. J. Linn. Soc. 177:937–949.

R Core Team. 2015. R: a language and environment for statistical computing. Vienna (Austria): R Foundation for Statistical Computing. Available from: URL https://www.R-project.org/.

Raj A., Stephens M., Pritchard J.K. 2014. Faststructure: variational inference of population structure in large SNP data sets. Genetics. 197:573.

Rambaut A., Suchard M., Xie D., Drummond A. 2014. Tracer v1.6. Available from: URL http://beast.bio.ed.ac.uk/Tracer.

Raupach M.J., Amann R., Wheeler Q.D., Roos C. 2016. The application of "-omics" technologies for the classification and identification of animals. Org. Divers. Evol. 16:1–12.

Rissler L.J., Apodaca J.J. 2007. Adding more ecology into species delimitation: ecological niche models and phylogeography help define cryptic species in the black salamander (*Aneides flavipunctatus*). Syst. Biol. 56:924–942.

Satler J.D., Carstens B.C., Hedin M. 2013. Multilocus species delimitation in a complex of morphologically conserved trapdoor spiders (Mygalomorphae, Antrodiaetidae, *Aliatypus*). Syst. Biol. 62:805–823.

Schlick-Steiner B.C., Steiner F.M., Seifert B., Stauffer C., Christian E., Crozier R.H. 2010. Integrative taxonomy: a multisource approach to exploring biodiversity. Annu. Rev. Entomol. 55:421–438.

Sherratt E., Gower D.J., Klingenberg C.P., Wilkinson M. 2014. Evolution of cranial shape in caecilians (Amphibia: Gymnophiona). Evol. Biol. 41:528.

Shirley M.H., Vliet K.A., Carr A.N., Austin J.D. 2014. Rigorous approaches to species delimitation have significant implications for African crocodilian systematics and conservation. Proc. Biol. Sci. 281:20132483.

Shoo L.P., Rose R., Doughty P., Austin J.J., Melville J. 2008. Diversification patterns of pebble-mimic dragons are consistent with historical disruption of important habitat corridors in arid Australia. Mol. Phylogenet. Evol. 48:528–542.

Singhal S., Hoskin C.J., Couper P., Potter S., Moritz C. 2018. A Framework for resolving cryptic species: a case study from the lizards of the Australian Wet Tropics. Syst. Biol. 67:1061–1075.

Smith K.L., Harmon L.J., Shoo L.P., Melville J. 2011. Evidence of constrained phenotypic evolution in a cryptic species complex of agamid lizards. Evolution. 65:976–992.

Smith W.J.S., Osborne W.S., Donnellan S.C., Cooper P.D. 1999. The systematic status of earless dragon lizards, *Tympanocryptis* (Reptilia: Agamidae), in south-eastern Australia. Aust. J. Zool. 47:551–564.

Sobral G., Hipsley C.A., Müller J. 2012. Braincase redescription of Dysalotosaurus lettowvorbecki (Dinosauria, Ornithopoda) based on computed tomography. Journal of Vertebrate Paleontology, 32:1090–1102.

Solís-Lemus C., Knowles L.L., Ané C. 2015. Bayesian species delimitation combining multiple genes and traits in a unified framework. Evolution. 69:492–507.

Spoor F., Wood B., Zonneveld F. 1994. Implications of early hominid labyrinthine morphology for evolution of human bipedal locomotion. Nature. 369:645.

Stamatakis A. 2014. RaxML version 8: a tool for phylogenetic analysis and post-analysis of large phylogenies. Bioinformatics. 30:1312–1313.

Stoev P., Komerički A., Akkari N., Liu S., Zhou X., Weigand A.M., Hostens J., Hunter C.I., Edmunds S.C., Porco D., Zapparoli M., Georgiev T., Mietchen D., Roberts D., Faulwetter S., Smith V., Penev L. 2013. *Eupolybothrus cavernicolus komerièki* & *stoev* sp. n. (Chilopoda: Lithobiomorpha: Lithobiidae): the first eukaryotic species description combining transcriptomic, DNA barcoding and micro-CT imaging data. Biodivers. Data J. 2013 (1):e1013.

Tan D.S., Ang Y., Lim G.S., Ismail M.R.B., Meier R. 2010. From 'cryptic species' to integrative taxonomy: an iterative process involving DNA sequences, morphology, and behaviour leads to the resurrection of *Sepsis pyrrhosoma* (Sepsidae: Diptera). Zool. Scr. 39:51–61.

Van Tassell C.P., Smith T.P.L., Matukumalli L.K., Taylor J.F., Schnabel R.D., Lawley C.T., Haudenschild C.D., Moore S.S., Warren W.C., Sonstegard T.S. 2008. SNP discovery and allele frequency estimation by deep sequencing of reduced representation libraries. Nat. Methods. 5:247–252.

Vogler A., Monaghan M. 2007. Recent advances in DNA taxonomy. J. Zool. Syst. Evol. Res. 45:1–10.

Wielstra B., Arntzen J.W. 2014. Exploring the effect of asymmetric mitochondrial DNA introgression on estimating niche divergence in morphologically cryptic species. PLoS One. 9:e95504.

Wiens J.J., Penkrot T.A. 2002. Delimiting species using DNA and morphological variation and discordant species limits in spiny lizards (*Sceloporus*). Syst. Biol. 51:69–91.

Wiens J.A., Rotenberry J.T. 1980. Patterns of morphology and ecology in grassland and shrubsteppe bird populations. Ecol. Monogr. 50:287–308.

Will K.W., Rubinoff D. 2004. Myth of the molecule: DNA barcodes for species cannot replace morphology for identification and classification. Cladistics. 20:47–55.

Wright S. 1978. Evolution and the genetics of populations: a treatise in four volumes: Vol. 4: Variability within and among natural populations. Chicago: The University of Chicago Press.

Yang Z., Rannala B. 2010. Bayesian species delimitation using multilocus sequence data. Proc. Nat. Acad. Sci. USA. 107:9264–9269.